Liquid Crystals
Publication details, including instructions for authors and subscription information:
http://www.informaworld.com/smpp/title~content=t713926090

Ferroelectric liquid crystals with fluoro- and aza-fluorenone cores: the effect of stereo-polar coupling

Adam J. McCubbin[a]; Victor Snieckus[a]; Robert P. Lemieux[a]
[a] Department of Chemistry, Queen's University, Kingston, Ontario, Canada K7L 3N6

To cite this Article McCubbin, Adam J. , Snieckus, Victor and Lemieux, Robert P.(2005) 'Ferroelectric liquid crystals with fluoro- and aza-fluorenone cores: the effect of stereo-polar coupling', Liquid Crystals, 32: 9, 1195 — 1203
To link to this Article: DOI: 10.1080/02678290500329408
URL: http://dx.doi.org/10.1080/02678290500329408

Liquid Crystals, Vol. 32, No. 9, September 2005, 1195–1203

Taylor & Francis
Taylor & Francis Group

Ferroelectric liquid crystals with fluoro- and aza-fluorenone cores: the effect of stereo-polar coupling

J. ADAM MCCUBBIN, VICTOR SNIECKUS and ROBERT P. LEMIEUX*
Department of Chemistry, Queen's University, Kingston, Ontario, Canada K7L 3N6

(*Received 25 February 2005; accepted 21 July 2005*)

The chiral fluorenone mesogens (*R*)-1-fluoro-2-(2-octyloxy)-7-(4-undecyloxybenzoyloxy)-fluoren-9-one (**2**) and (*R*)-2-(2-octyloxy)-7-(4-undecyloxybenzoyloxy)-3-azafluoren-9-one (**3**) were synthesized using a combined *ortho*-directed and remote metalation strategy, which also incorporates a Suzuki–Miyaura crosscoupling step. These compounds form chiral SmC* liquid crystal phases with reduced polarizations ($\mathbf{P}_o$) of +475 and +332 nC cm^{-2} at 10 K below the Curie point, respectively. These values are considerably larger than that previously reported for the unsubstituted fluorenone (*R*)-2-(2-octyloxy)-7-(4-undecyloxybenzoyloxy)-fluoren-9-one (**1**), which is +111 nC cm^{-2} at 10 K below the Curie point. Molecular modelling based on the Boulder model suggests that the larger polarizations result from a conformational bias of the fluorenone core dipole moment along the polar axis of the SmC* phase caused by stereo-polar coupling with the chiral 2-octyloxy side chain.

1. Introduction

The spontaneous polarization ($\mathbf{P}_S$) in ferroelectric liquid crystals originates from a conformational preference of transverse molecular dipoles to orient in one direction along the polar axis of the SmC* phase, due to steric coupling between polar functional groups and the stereogenic centre(s) (stereo-polar coupling). Empirical and semiempirical structure–property relationships based on conformational analysis of such stereo-polar units are well established for SmC* mesogens with chiral side chains such as the 2-octyloxy group [1–3]. In such mesogens, the introduction of a substituent *ortho* to a 2-octyloxy side chain strengthens the coupling of the aromatic core to the chiral side chain and normally results in higher spontaneous polarizations, especially if the *ortho* substituent is polar [4–7]. In this paper, we show how this strategy can produce significant increases in the spontaneous polarization of a SmC* mesogen by coupling a chiral (*R*)-2-octyloxy side chain to a polar fluorenone core.

Very few examples of fluorenone liquid crystals have been reported [8–12]. Recently, we reported the synthesis and characterization of a series of ferroelectric SmC* liquid crystals with a fluorenone core (e.g. (*R*)-2-(2-octyloxy)-7-(4-undecyloxybenzoyloxy)fluoren-9-one, **1**) using a combined directed *ortho* metalation (D*o*M)–directed remote metalation (DreM) strategy [12]. Molecular modelling based on the Boulder model suggests that the fluorenone core is weakly coupled to the chiral (*R*)-2-octyloxy side chain due to the bent shape of the core, which restricts its free rotation with respect to the side chain while maintaining the zigzag shape imposed by the ordering of the SmC* phase [2]. To increase the spontaneous polarization of the SmC* phase formed by **1**, stereo-polar coupling of the fluorenone core to the chiral side chain was enhanced by two different structural modifications: (i) introduction of a fluoro group *ortho* to the chiral side chain, and (ii) substitution of a heterocyclic nitrogen for the fluorenone carbon at C-3. Herein, we describe the syntheses of the fluoro-substituted fluorenone **2** and azafluorenone **3**, and the determination of their mesogenic and ferroelectric properties.

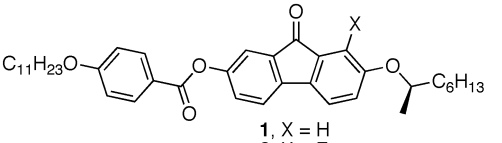

1, X = H
2, X = F

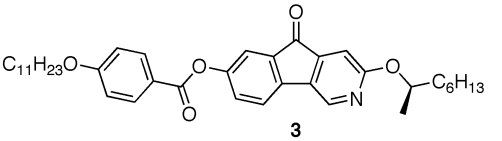

3

*Corresponding author. Email: lemieux@chem.queensu.ca

Liquid Crystals
ISSN 0267-8292 print/ISSN 1366-5855 online © 2005 Taylor & Francis
http://www.tandf.co.uk/journals
DOI: 10.1080/02678290500329408

2. Results and discussion

2.1. *Synthesis*

Compounds **2** and **3** were synthesized using a modification of the route first reported for **1** (scheme 1) [12]. In order to provide a readily cleavable protective group downstream in the synthesis, the methyl ether **4** was treated with BBr_3 to give **5**, which was converted into the MOM ether **6**. The more reactive D*o*M site of **6** was protected by metalation–silylation to give **7**. A second D*o*M at higher temperature followed by quenching of the resulting carbanion with $B(OMe)_3$ gave the corresponding boronic acid, which was converted into the pinacol ester **8** for purification by column chromatography. The coupling partner precursors **9a** and **9b** were functionalized directly with (*S*)-2-octanol via a Mitsunobu reaction to give **10a** and **10b**, which were subjected to Suzuki–Miyaura crosscoupling with **8** to give **11a** and **11b**. Desilylation using tetrabutylammonium fluoride (TBAF) afforded **12a** and **12b**. Directed remote metalation (DreM) using lithium dimethylamide (LDA) proceeded with high regioselectivity to give the fluorenones **13a** and **13b**, respectively, without detectable amounts of the other regioisomers. The regioselectivity of cyclization in **12a** is consistent with that observed previously in similar substrates [13–15]. The cooperative effect of *meta*-related fluoro and amide DMGs to direct metalation *in between*, as in **12a**, has been previously established [16]. The regioselectivity of cyclization in **12b** may be governed by pyridine C-4 acidity in conjunction with the orientation of an amide-LDA complex of the twisted azabiaryl derivative; complex-induced proximity effect (CIPE) [13]. MOM deprotection with HCl furnished **14a** and **14b** which,

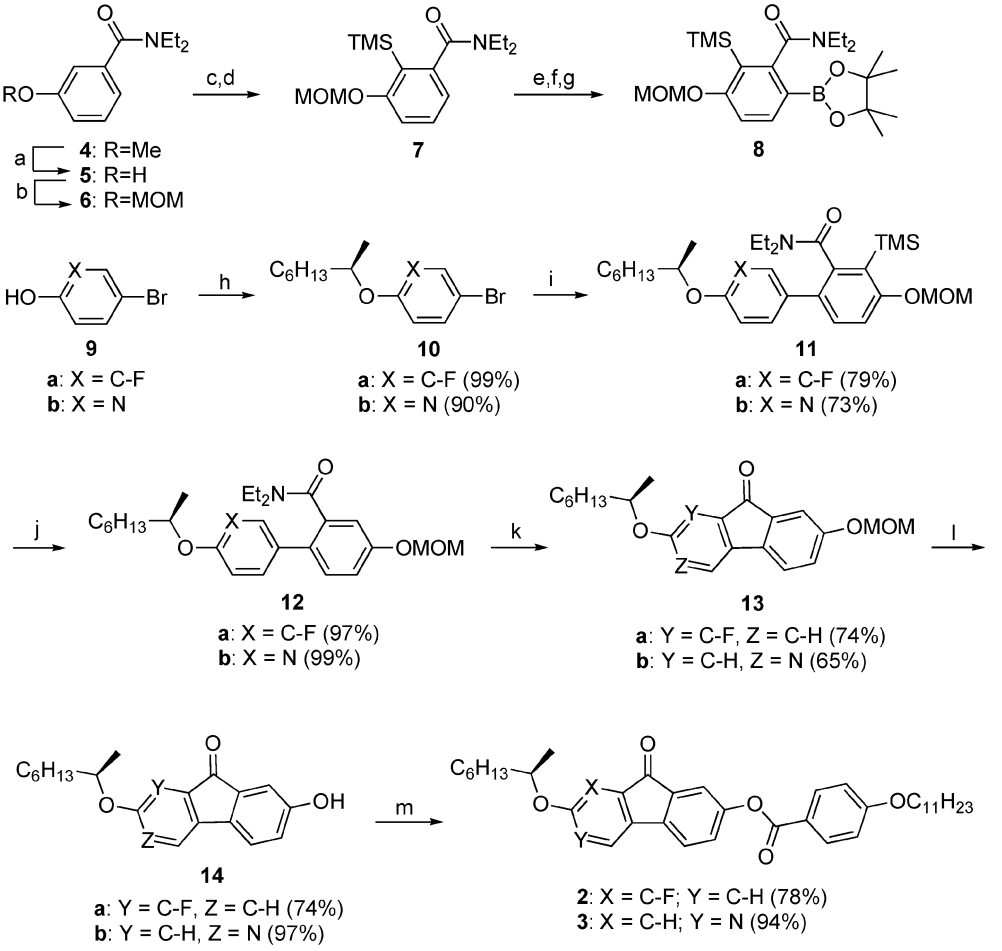

Scheme 1. *Reagents and conditions:* (a) BBr_3, CH_2Cl_2, −78°C to 25°C (98%); (b) MOMCl, CH_2Cl_2, *i*-Pr_2NEt, 0°C to 25°C (83%); (c) *s*-BuLi, TMEDA, THF, −78°C (d) TMSCl, −78°C to 25°C (75%); (e) *s*-BuLi, TMEDA, THF, −10°C; (f) $B(OMe)_3$, −10°C to 25°C; (g) pinacol (60%); (h) (*S*)-2-octanol, PPh_3, DIAD, CH_2Cl_2, 25°C; (i) **8**, $Pd(PPh_3)_4$, $K_2CO_{3(aq)}$, DME, reflux; (j) TBAF, THF, 25°C; (k) LDA, THF, 0°C to 25°C; (l) $HCl_{(aq)}$, *i*-PrOH, 25°C; (m) DCC, DMAP, 4-undecyloxybenzoic acid CH_2Cl_2, 25°C.

upon esterification with 4-undecyloxybenzoic acid using DCC and DMAP, gave the mesogens **2** and **3** in 10 steps and 12 and 16% overall yield, respectively.

2.2. *Mesophase characterization*

The mesophases formed by **2** and **3** were characterized by polarizing optical microscopy (POM), differential scanning calorimetry (DSC) and powder X-ray diffraction (XRD) (Table 1). Both compounds form an enantiotropic SmC* phase, as shown by the broken fan textures and pseudo-homeotropic domains in figure 1. The SmC* phases formed by **2** and **3** have broader temperature ranges and higher clearing points than that formed by the unsubstituted **1**, which may be ascribed to stronger dipole–dipole interactions between the polar fluorenone cores. Further analysis by powder XRD confirmed the SmC* phase assignments for **2** and **3**. In each case, a single sharp Bragg peak was observed at $2\theta = 2.92^\circ$ and 2.66°, which correspond to layer spacings of 30.3 and 33.2 Å, respectively, with a broad halo at wide angles. The Bragg angle for the small angle peak remains constant over broad temperature ranges in the SmC* phase (90–110°C for **2**, 70–90°C for **3**). The layer spacings are shorter than the calculated molecular lengths for **2** and **3** (35.9 and 36.3 Å), which is consistent with a tilted lamellar structure with tilt angles of 32° and 24°, respectively.

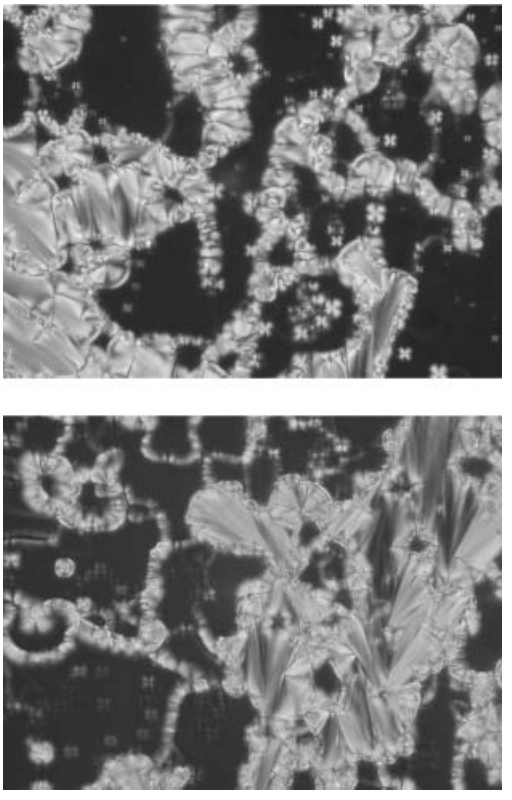

Figure 1. Photomicrographs of **2** in the SmC* phase at 96°C (500 ×, top) and **3** in the SmC* phase at 98°C (500 ×, bottom).

2.3. *Polarization measurements*

Spontaneous polarizations ($\mathbf{P}_S$) and tilt angles (θ) of the SmC* phases formed by **2** and **3** were measured as a function of temperature (figure 2). For comparison, $\mathbf{P}_S$ and θ values for **1**–**3** at $T - T_C = -10$ K are listed in table 1, along with the corresponding reduced polarization values ($\mathbf{P}_o$) According to phenomenological theory, the spontaneous polarization $\mathbf{P}_S$ and tilt angle θ of a SmC* phase are related to the reduced polarization $\mathbf{P}_o$ according to the equation $\mathbf{P}_o = \mathbf{P}_S(\sin\theta)^{-1}$. The reduced polarization is intrinsic to the chiral component of the SmC* phase at a fixed reduced temperature $T - T_C$ [17].

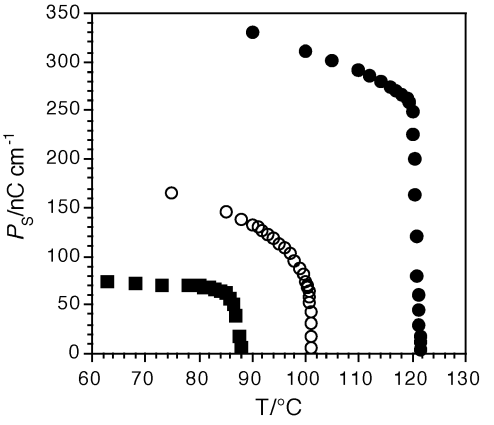

Figure 2. Spontaneous polarization $\mathbf{P}_S$ as a function of temperature T for the unsubstituted fluorenone **1** (squares), fluoro-substituted fluorenone **2** (filled circles) and azafluorenone **3** (open circles).

Table 1. Liquid crystalline and ferroelectric properties of compounds **1**, **2** and **3**.

Compound	Phase sequence[a]					$\mathbf{P}_s$/nC cm^{-2}[b]	θ/deg[b]	$\mathbf{P}_o$/nC cm^{-2}[b]
1[c]	Cr	62 (35.0)	SmC*	87 (6.5)	I	+70	39	+111
2	Cr	84 (54.1)	SmC*	119 (7.2)	I	+286	37	+475
3	Cr	65 (42.4)	SmC*	101 (6.6)	I	+130	23	+332

[a]Phase transition temperatures in °C and enthalpies of transition in kJ mol^{-1} (in parentheses) were measured on heating by DSC at a rate of 5 K min^{-1}. [b]Measured at a reduced temperature of $T - T_C = -10$ K. [c]From [12].

The tilt angles measured by POM are in excellent agreement with those derived from XRD measurements, and found to be invariant with temperature. The $\mathbf{P}_o$ values of the fluoro-substituted fluorenone **2** and azafluorenone **3** are significantly larger than that previously reported for the unsubstituted fluorenone **1**, which is consistent with a higher degree of stereo-polar coupling between the 2-octyloxy side chain and the polar fluorenone core.

3. Molecular modelling

The polar ordering of the fluorenone core in **1**–**3** relative to the (*R*)-2-octyloxy side chain was modelled at the AM1 level according to the Boulder model [2, 3]. Hence, the SmC* mesogens were assumed to adopt a zigzag conformation in which the fluorenone core is more tilted than the side chains. The lowest energy conformation of the (*R*)-2-octyloxy side chain features a *gauche* bend about the bond joining C-2 and C-3, which gives an orientation of the alkoxy dipole along the polar axis that is consistent with the positive sign of $\mathbf{P}_s$ observed experimentally for **1**–**3**. As shown in figure 3, the lowest energy conformations of the three mesogens are approximately isosteric, and therefore provide a useful basis for comparison. Starting from these conformations, the fluorenone cores were rotated 180° with respect to the two side chains and the molecules minimized again to give, in each case, conformations **a** and **b** with opposite core orientations along the polar axis. These conformational distributions are oversimplifications of a complex conformational/orientational hypersurface, but they can provide a useful basis to understand the molecular origins of $\mathbf{P}_s$. To assess qualitatively the changes in molecular shape and transverse dipole moment ($\mu_\perp$) upon core rotation, the 4-alkoxybenzoyl units were oriented in the *xy*-plane corresponding to the SmC* tilt plane, and $\mu_\perp$ values along the polar *z*-axis were calculated at the AM1 level. In the case of the unsubstituted fluorenone **1**, the two conformations **1a** and **1b** have approximately the same energy and very similar shapes conforming to the zigzag binding site of the Boulder model, which suggests that neither core orientation is strongly favoured in the SmC* phase formed by **1**, and that the fluorenone dipole makes a relatively small contribution to $\mathbf{P}_s$. This is consistent with the similarity of the reduced polarization of **1** to those reported for conventional mesogens with (*R*)-2-octyloxy side chains as the only stereo-polar unit [2].

A comparison of conformations **2a** and **2b** reveals a significant conformational bias of the fluoro-substituted fluorenone core with respect to the chiral side chain by virtue of a strong stereo-polar coupling between the alkoxy and *ortho*-fluoro groups. In the lowest energy zigzag conformation **2a**, the alkoxy group is *anti*-periplanar relative to the fluoro group; a 180° rotation of the fluorenone core forces the chiral side chain out of the tilt plane—well outside the spatial boundaries of the Boulder model binding site—due to the absence of a

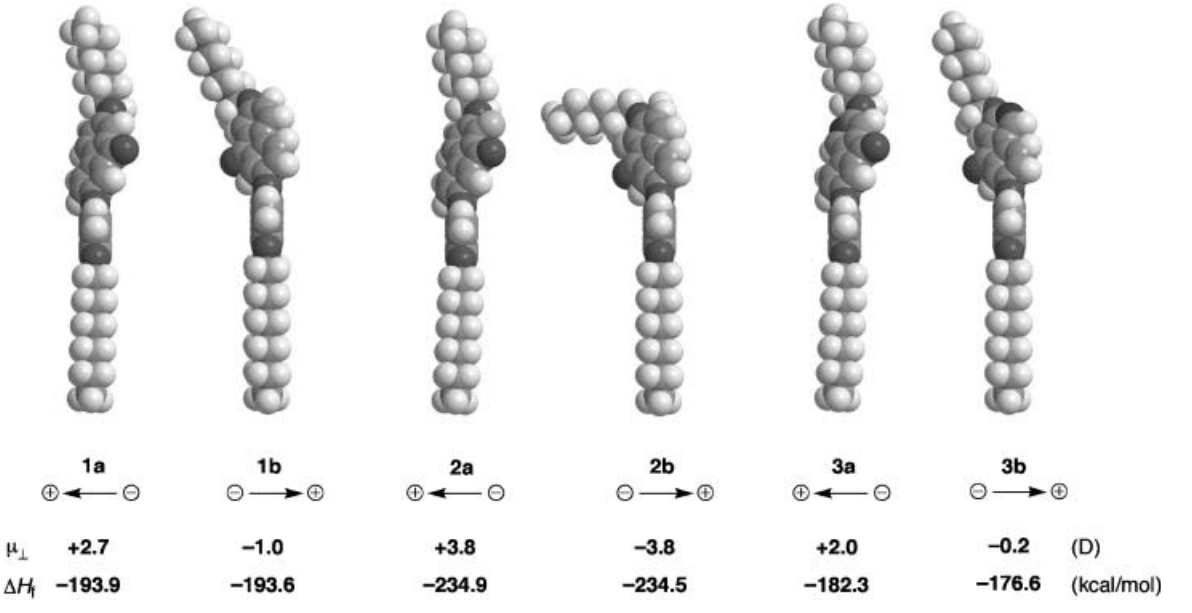

Figure 3. Space-filling models showing minimized zigzag conformations of mesogens **1**–**3** as end-on views. The heats of formations (ΔH_f) and transverse dipole moments ($\mu_\perp$) were calculated for each minimized structure at the AM1 level. The tilt plane is vertical, normal to the plane of the page, and the polar axis is horizontal, in the plane of the page.

local energy minimum in which the alkoxy group is *syn*-periplanar relative to the fluoro group (**2b**). This inability to conform to the order imposed by the SmC* phase, as modelled by the zigzag binding site of the Boulder model, makes conformation **2b** less favourable even though the AM1 calculations predict that **2a** and **2b** should have virtually the same energy in the gas phase. In conformation **2a**, the alkoxy dipole of the chiral side chain is coupled to that of the fluoro-substituted fluorenone core to give a large transverse dipole moment of +3.8 D. The increase in $\mu_\perp$ relative to that of **1** in the same isosteric conformation (+2.7 D), combined with a greater conformational bias of the fluoro-substituted fluorenone core relative to the chiral side chain, is consistent with the 4-fold increase in spontaneous polarization achieved with mesogen **2**.

In the azafluorenone **3**, rotation of the core with respect to the side chains has relatively little effect on the zigzag shape of the mesogen, because energy minima exist for the two conformations **3a** and **3b** in which the alkoxy group is either *syn*- or *anti*-periplanar with respect to the heterocyclic nitrogen. In this case, stereo-polar coupling is manifested in the difference in ΔH_f values which favours the less sterically congested *syn*-periplanar conformation. However, this conformational bias is achieved at the expense of the transverse dipole moment, which is lower for the azafluorenone core of **3**. The net result is a spontaneous polarization that is intermediate between that of **1**, in which a more polar fluorenone core is decoupled from the chiral side chain, and that of **3**, in which a much more polar fluoro-substituted fluorenone core is coupled to the chiral side chain.

4. Conclusions

The synthesis of fluoro-substituted fluorenone and azafluorenone SmC* mesogens has been achieved by a combined regioselective *ortho*-directed and remote metalation strategy which is interspersed by a Suzuki–Miyaura crosscoupling step. Increased stereo-polar coupling between the core and the chiral 2-octyloxy side chain, due to the presence of a fluoro substituent or heterocyclic nitrogen, resulted in significant increases in spontaneous polarization relative to the unsubstituted parent compound, in which the fluorenone core is more or less decoupled from the chiral side chain.

5. Experimental

5.1. *Characterization*

^{1}H (400 MHz) and ^{13}C (100 MHz) NMR spectra were recorded on a Bruker AV-400 spectrometer in $CDCl_3$ (unless otherwise indicated). The chemical shifts are reported in δ (ppm) relative to tetramethylsilane or $CDCl_3$ as internal standard. Low resolution mass spectra were recorded on a Micromass VG Quattro triple quadrupole mass spectrometer; peaks are reported as *m*/*z* (percent intensity relative to the base peak). High resolution mass spectra were recorded on a Micromass 70–250S double focusing mass spectrometer. Infrared spectra were recorded on a Bomem MB-100 FTIR spectrometer with samples as KBr pellets or neat on NaCl plates. Melting points were obtained using a Fisher Scientific hot stage apparatus and are uncorrected. Differential scanning calorimetry analyses were performed on a Perkin-Elmer DSC-7 instrument with a scanning rate of $5\,K\,min^{-1}$. Texture analyses were performed using a Nikon Eclipse E600 POL polarizing microscope fitted with a Linkam LTS 350 hot stage and TMS 93 temperature controller. Variable temperature powder X-ray diffraction analyses were performed at the Centre de Recherche en Sciences et Ingénierie des Macromolécules (CERSIM) of Université Laval using a Siemens/Bruker Kristalloflex 760 diffractometer fitted with a Hi-Star bidimensional detector (Cu K_α radiation, λ=1.5418 Å). Molecular modelling calculations were carried out at the AM1 level using MOPAC 97 as implemented on Chem3D Pro, version 4.0 (CambridgeSoft).

Spontaneous polarizations ($\mathbf{P}_S$) were measured as a function of temperature by the triangular wave method ($10–15\,V\,\mu m^{-1}$, 80–100 Hz) using a Displaytech APT-III polarization testbed in conjunction with the Linkam hot stage [18]. Rubbed polyimide-coated ITO glass cells with a 4 μm spacing (Displaytech Inc.) were used for all measurements. Alignment of the SmC* phase was achieved by slow cooling ($0.1\,K\,min^{-1}$) from the isotropic phase while applying an a.c. field (4 Hz, $5\,V\,\mu m^{-1}$) across the film. Tilt angles (θ) were measured by polarizing microscopy as half the rotation between two extinction positions corresponding to opposite signs of the applied field. The sign of $\mathbf{P}_S$ along the polar axis was assigned from the relative configuration of the electric field and the switching position of the sample according to the established convention [2].

5.2. *Synthesis*

5.2.1. N,N-Diethyl 3-hydroxybenzamide (5). To a solution of **4** [12] (27.4 g, 132 mmol) in CH_2Cl_2(500 ml) cooled to −78°C under argon was added dropwise neat BBr_3 (31.3 ml, 2.5 equiv). The mixture was stirred for 30 min at −78°C, then allowed to warm to room temperature over 30 min. The reaction mixture was cooled to 0°C, neutralized with saturated aq Na_2CO_3, diluted with water and extracted twice with CH_2Cl_2. The combined organic layers were extracted with 10%

aq NaOH. The aqueous extract was neutralized with 2M aq HCl, extracted twice with CH_2Cl_2 and the combined organic extracts were dried ($MgSO_4$) and concentrated to give 24.9 g (98%) of **5** as a colourless solid: m.p. 81–82°C (EtOAc) (lit. [19] 84°C); ^{1}H NMR (400 MHz, $CDCl_3$) δ 7.12 (dd, ^3J=8.0 Hz, ^3J=8.0 Hz, 1H), 6.84 (m, 1H), 6.76 (m, 2H), 3.52 (m, 2H), 3.24 (m, 2H), 1.23 (m, 3H), 1.08 (m, 3H).

5.2.2. N,N-Diethyl 3-methoxymethoxybenzamide (6). Under an Ar atmosphere, MOMCl (11.4 ml, 1.1 equiv) was added dropwise to a solution of **5** (26.4 g, 137 mmol) and *i*-Pr_2NEt (48.8 mL, 2.0 equiv) in dry CH_2Cl_2 (500 ml) cooled to 0°C. The mixture was stirred for 4 h at room temperature, diluted with water and extracted twice with CH_2Cl_2. The combined organic extracts were dried ($MgSO_4$) and concentrated to give a yellow oil. Purification by flash chromatography on silica gel (20% EtOAc/hexanes) gave 27.0 g (83%) of **6** as a colourless oil: IR (KBr) 1633 cm^{-1}; ^{1}H NMR (400 MHz, $CDCl_3$) δ 7.35 (dd, ^3J=9.1 Hz, ^{4}J=7.8 Hz, 1H), 7.08 (m, 3H), 5.23 (s, 2H), 3.60 (m, 2H), 3.52 (s, 3H), 3.34 (m, 2H), 1.25 (m, 6H); ^{13}C NMR (100 MHz, $CDCl_3$) δ 170.8, 157.2, 138.6, 129.6, 119.6, 117.0, 114.2, 94.4, 55.9, 43.3, 39.2, 14.1, 12.9; MS (EI) *m*/*z* 237 (M^+, 51), 165 (100) 135 (14); HRMS (EI) calcd for $C_{13}H_{19}NO_3$: 237.1365, found 237.1366.

5.2.3. N,N-Diethyl 3-methoxymethoxy-2-trimethylsilyl-benzamide (7). To a dry flask containing **6** (17.0 g, 72 mmol) and TMEDA (13.0 ml, 1.2 equiv) in dry THF (500 ml) cooled to −78°C under argon was added *s*-BuLi as a 1.1 M solution in hexane (78.1 ml, 1.2 equiv). After the mixture was stirred at −78°C for 1 h, TMSCl (10.9 ml, 1.2 equiv) was added dropwise and the mixture allowed to warm to room temperature over 2 h. The mixture was diluted with saturated aq NH_4Cl, concentrated and extracted twice with EtOAc. The combined organic extracts were washed with brine, dried ($MgSO_4$) and concentrated to give a yellow oil. Purification by flash chromatography on silica gel (15% EtOAc/hexanes) gave 16.7 g (75%) of **7** as a colourless oil: IR (KBr) 1635 cm^{-1}; ^{1}H NMR (400 MHz, $CDCl_3$) δ 7.22 (dd, ^3J=8.4 Hz, ^3J=7.6 Hz, 1H), 6.99 (d, J=8.4 Hz, 1H), 6.71 (d, J=7.6 Hz, 1H), 5.04 (s, 2H), 3.63 (m, 1H), 3.40 (s, 3H), 3.38 (m, 1H), 3.21 (m, 2H), 1.18 (t, J=7.2 Hz, 3H), 0.99 (t, J=7.2 Hz, 3H), 0.21 (s, 9H); ^{13}C NMR (100 MHz, $CDCl_3$) δ 171.6, 162.6, 144.5, 130.4, 124.5, 119.3, 112.5, 94.0, 56.0, 43.3, 38.8, 13.6, 12.7, 0.4; MS (EI) *m*/z 310 (M^+, 23), 294 (100), 278 (12), 250 (58); HRMS (EI) calcd for $C_{16}H_{27}NO_3Si$: 310.1838, found 310.1848.

5.2.4. 2-N,N-Diethylcarbamoyl-4-methoxymethoxy-3-trimethylsilylphenylboronic acid pinacol ester (8). To a dry flask containing **7** (16.7 g, 53.8 mmol) and TMEDA (16.2 ml, 2.0 equiv) in dry Et_2O (500 ml) cooled to −10°C under argon was added *s*-BuLi as a 1.0 M solution in hexane (108 ml, 2.0 equiv). After the mixture was stirred at −10°C for 2 h, $B(OMe)_3$ (12.2 ml, 2.0 equiv) was added rapidly and the mixture allowed to warm to room temperature over 2 h. The mixture was diluted with saturated aq NH_4Cl, concentrated and extracted twice with EtOAc. The combined organic extracts were washed with brine and dried ($MgSO_4$). To this solution was added pinacol (12.7 g, 2.0 equiv), and the mixture was concentrated to afford a yellow oil. Purification by flash chromatography on silica gel (10% EtOAc/hexanes) gave 14.1 g (60%) of **8** as a colourless oil: IR (KBr) 1637 cm^{-1}; ^{1}H NMR (400 MHz, $CDCl_3$) δ 7.78 (d, J=8.3 Hz, 1H), 6.97 (d, J=8.3 Hz, 1H), 5.15 (s, 2H), 3.67 (m, 1H), 3.42 (s, 3H), 3.24 (s, 3H), 3.08 (m, 2H), 1.23 (m, 15H), 0.97 (m, 3H), 0.24 (s, 9H); ^{13}C NMR (100 MHz, $CDCl_3$) δ 171.3, 165.1, 150.8, 139.7, 124.1, 111.6, 94.2, 83.7, 56.4, 43.5, 39.5, 25.1, 24.8, 13.4, 12.7, 1.0; MS (EI) *m*/*z* 435 (M^+, 24), 420 (79), 376 (21), 362 (68), 45 (100); HRMS (EI) calcd for $C_{22}H_{38}BNO_4Si$: 436.2691, found 436.2688.

5.2.5. (*R*)-4-Bromo-2-fluoro-1-(2-octyloxy)benzene (10a). Under an Ar atmosphere, DIAD (3.1 ml, 1.5 equiv) was added dropwise to a solution of **9a** (2.0 g, 10.5 mmol, Aldrich), (*S*)-2-octanol (1.5 g, 1.1 equiv) and Ph_3P (3.3 g, 1.2 equiv) in CH_2Cl_2 (100 ml) at room temperature. The mixture was stirred for 4 h, diluted with water and extracted twice with CH_2Cl_2. The combined organic extracts were dried ($MgSO_4$) and concentrated to afford a yellow oil. Purification by flash chromatography on silica gel (10% EtOAc/hexanes) gave 3.13 g (99%) of **10a** as a colourless oil: IR (KBr) 1497, 1268 cm^{-1}; ^{1}H NMR (400 MHz, $CDCl_3$) δ 7.22 (dd, ^3J=7.3 Hz, ^4J=2.5 Hz, 1H), 7.15 (m, 1H), 6.83 (t, J=7.3 Hz, 1H), 4.30 (m, 1H), 1.72 (m, 1H), 1.57 (m, 1H), 1.28 (m, 11H), 0.88 (m, 3H); ^{13}C NMR (100 MHz, $CDCl_3$) δ 155.2, 152.7, 145.9, 127.4, 120.2, 119.0, 77.0, 36.7, 32.1, 29.5, 25.7, 22.9, 19.9, 14.3; MS (EI) *m*/*z* 304 ($(M+2)^+$, 4), 303 ($(M+1)^+$, 2), 302 (M^+, 4), 190 (100), 83 (50); HRMS (EI) calcd for $C_{14}H_{20}BrFO$: 302.0682, found 302.0681.

5.2.6. (*R*)-5-Bromo-2-(2-octyloxy)pyridine (10b). The procedure described for the synthesis of **10a** was repeated with **9b** (1.82 g, 10.5 mmol, Aldrich) to give 1.69 g (90%) of **10b** as a colourless oil: IR (KBr) 1583, 1463 cm^{-1}; ^{1}H NMR (400 MHz, $CDCl_3$) δ 8.15 (s, 1H), 7.57 (d, J=8.8 Hz, 1H), 6.57 (d, 8.8 Hz, 1H), 5.11 (m, 1H), 1.52 (m, 13H), 0.86 (m, 3H); ^{13}C NMR (100 MHz,

$CDCl_3$) δ 162.9, 147.8, 141.3, 113.5, 111.2, 72.4, 36.5, 32.1, 29.6, 25.8, 22.9, 20.1, 14.4; MS (EI) *m/z* 287 ($(M+2)^+$, 2), 286 ($(M+1)^+$, 1), 285 (M^+, 2), 173 (100), 145 (31); HRMS (EI) calcd for $C_{13}H_{20}BrNO$: 285.0728, found 285.0741.

5.2.7. (*R*)-N,N-Diethyl 3′-fluoro-4-methoxymethoxy-4′-(2-octyloxy)-3-trimethylsilylbiphenyl-2-carboxamide (11a). In a 2-neck flask fitted with a reflux condenser kept under Ar were sequentially added a solution of **8** (4.51 g, 10.4 mmol) in degassed DME (100 ml), $Pd(PPh_3)_4$ (598 mg, 0.050 equiv), **10a** (3.13 g, 1.0 equiv) and a 2M aq solution of K_2CO_3 (15.5 ml, 3.0 equiv). The mixture was heated under reflux for 12 h, cooled, and extracted twice with EtOAc. The combined organic extracts were washed with saturated aq NH_4Cl, brine, dried ($MgSO_4$) and concentrated to afford a brown oil. Purification by flash chromatography on silica gel (10% EtOAc/hexanes) gave 4.35 g (79%) of **11a** as a colourless oil: IR (KBr) 1632 cm^{-1}; ^1H NMR (400 MHz, $CDCl_3$) δ 7.24 (d, J=8.6 Hz, 1H), 7.14 (m, 3H), 6.92 (m, 1H), 5.21 (s, 2H), 4.34 (m, 1H), 3.82 (m, 1H), 3.51 (s, 3H), 2.96 (m, 1H), 2.72 (m, 2H), 1.30 (m, 13H), 0.88 (m, 3H), 0.79 (m, 6H), 0.31 (s, 9H); ^{13}C NMR (100 MHz, $CDCl_3$) δ 169.9, 162.5, 152.1, 145.5, 142.7, 134.0, 132.6, 131.1, 125.7, 125.4, 117.9, 117.7, 113.0, 94.5, 77.0, 56.5, 42.9, 38.5, 36.7, 32.1, 29.6, 25.7, 22.9, 20.1, 14.4, 13.2, 12.0, 1.1; MS (EI) *m/z* 531 (M^+, 13), 516 (79), 500 (18), 404 (100), 360 (27), 45 (64); HRMS (EI) calcd for $C_{30}H_{46}FNO_4Si$: 531.3180, found 531.3185.

5.2.8. (*R*)-N, N-Diethyl 3-methoxymethoxy-6-[6-(2-octyloxy)pyridin-3-yl]-2-trimethylsilylbenzamide (11b). The procedure described for the synthesis of **11a** was repeated with **8** (2.58 g, 5.92 mmol) and **10b** (1.69 g, 1.0 equiv) to give 2.13 g (73%) of **11b** as a colourless oil: IR (KBr) 1634 cm^{-1}; ^1H NMR (400 MHz, $CDCl_3$) δ 8.11 (s, 1H), 7.68 (d, J=8.3 Hz, 1H), 7.23 (d, J=8.6 Hz, 1H), 7.14 (d, J=8.6 Hz, 1H), 6.64 (d, J=8.3 Hz, 1H), 5.22 (s, 2H), 5.18 (m, 1H), 3.80 (m, 1H), 3.51 (s, 3H), 2.97 (m, 1H), 2.73 (m, 2H), 1.29 (m, 13H), 0.80 (m, 9H), 0.31 (s, 9H); ^{13}C NMR (100 MHz, $CDCl_3$) δ 169.9, 163.4, 162.6, 144.9, 142.2, 139.5, 132.7, 129.0, 125.5, 113.1, 110.7, 94.5, 66.2, 56.6, 42.8, 38.4, 36.7, 36.6, 32.2, 29.6, 25.8, 23.0, 20.3, 20.2, 15.6, 14.4, 13.2, 12.1, 1.1; MS (EI) *m/z* 514 (M^+, 7), 499 (100), 387 (65), 343 (27), 73 (47); HRMS (EI) calcd for $C_{29}H_{46}N_2O_4Si$: 514.3227, found 514.3231.

5.2.9. (*R*)-N,N-Diethyl 3′-fluoro-4-methoxymethoxy-4′-(2-octyloxy)biphenyl-2-carboxamide (12a). To a solution of **11a** (2.86 g, 5.38 mmol) in THF (50 ml) was added a 1M solution of TBAF in THF (10.8 ml, 2.0 equiv). The mixture was stirred for 12 h at 25°C, then diluted with saturated aq NH_4Cl, and the whole was concentrated and extracted twice with EtOAc. The combined organic extracts were washed with brine, dried ($MgSO_4$) and concentrated to afford a brown oil. Purification by flash chromatography on silica gel (25% EtOAc/hexanes) gave 2.41 g (97%) of **12a** as a colourless oil: IR (KBr) 1630 cm^{-1}; ^1H NMR (400 MHz, $CDCl_3$) δ 7.45 (dd, ^3J=8.6 Hz, ^4J=2.0 Hz, 1H), 7.29 (d, J=8.3 Hz, 1H), 7.18 (dd, ^3J=8.3 Hz, ^4J=2.9 Hz, 1H), 7.11 (d, J=2.5 Hz, 1H), 7.08 (dd, ^3J=8.6 Hz, ^4J=2.5 Hz, 1H), 7.03 (d, J=2.5 Hz, 1H), 5.25 (s, 2H), 4.36 (m, 1H), 3.81 (m, 1H), 3.49 (s, 3H), 2.99 (m, 2H), 2.74 (m, 1H), 1.79 (m, 1H), 1.60 (m, 1H), 1.31 (m, 11H), 0.97 (m, 3H), 0.89 (m, 3H), 0.81 (m, 3H); ^{13}C NMR (100 MHz, $CDCl_3$) δ 170.2, 157.0, 154.8, 152.4, 139.8, 137.6, 133.2, 130.9, 130.8, 129.1, 128.6, 127.5, 125.0, 117.1, 115.0, 94.8, 76.8, 56.4, 42.6, 38.7, 36.7, 32.1, 29.6, 25.7, 22.9, 20.1, 14.4, 13.7, 12.3; MS (EI) *m/z* 460 (M^+, 9), 345 (5), 314 (29), 275 (22), 139 (57), 72 (63), 45 (100); HRMS (EI) calcd for $C_{27}H_{38}FNO_4$: 459.2785, found 459.2790.

5.2.10. (*R*)-N, N-Diethyl 5-methoxymethoxy-2-[6-(2-octyloxy)pyridin-3-yl]benzamide (12b). The procedure described for the synthesis of **12a** was repeated with **11b** (1.06 g, 2.06 mmol). Purification by flash chromatography on silica gel (30% EtOAc/hexanes) gave 0.924 g (99%) of **12b** as a colourless oil: IR (KBr) 1632 cm^{-1}; ^1H NMR (400 MHz, $CDCl_3$) δ 8.15 (d, J=2.8 Hz, 1H), 7.68 (dd, ^3J=8.6 Hz, ^4J=2.8 Hz, 1H), 7.27 (d, J=8.6 Hz, 1H), 7.11 (dd, ^3J=8.6 Hz, ^4J=2.5 Hz, 1H), 7.05 (d, J=2.5 Hz, 1H), 6.66 (d, J=8.6 Hz, 1H), 5.24 (s, 2H), 5.18 (m, 1H), 3.77 (m, 1H), 3.49 (s, 3H), 3.00 (m, 2H), 2.78 (m, 1H), 1.31 (m, 10H, 1.21 (t, J=6.9 Hz, 3H), 0.94 (t, J=6.9 Hz, 3H), 0.87 (m, 6H); ^{13}C NMR (100 MHz, $CDCl_3$) δ 170.1, 163.4, 157.1, 146.4, 139.6, 138.0, 130.9, 128.9, 128.3, 117.2, 115.0, 111.1, 94.8, 72.1, 66.2, 56.4, 42.7, 38.8, 36.7, 32.1, 29.6, 25.8, 22.9, 20.2, 15.6, 14.4, 13.8, 12.5; MS (EI) *m/z* 432 (M^+, 10), 314 (7), 258 (8), 139 (28), 45 (100); HRMS (EI) calcd for $C_{26}H_{28}N_2O_4$: 442.2832, found 442.2829.

5.2.11. (*R*)-1-Fluoro-7-methoxymethoxy-2-(2-octyloxy) fluoren-9-one (13a). Under an Ar atmosphere, a freshly prepared 1.0 M solution of LDA in dry THF (26.2 ml, 5.0 equiv) was added dropwise to a solution of **12a** (2.41 g, 5.25 mmol) in dry THF (250 ml) cooled to 0°C. After the mixture was stirred at room temperature for 12 h, saturated aq NH_4Cl solution was added and the mixture was extracted twice with Et_2O. The combined organic extracts were washed with brine, dried ($MgSO_4$) and concentrated to give a red oil. Purification by flash chromatography on silica gel (5% EtOAc/hexanes)

afforded 1.49 g (74%) of **13a** as an orange oil: IR (KBr) 1718 cm^{-1}; ^1H NMR (400 MHz, $CDCl_3$) δ 7.30 (d, J=8.4 Hz, 1H), 7,29 (s, 1H), 7.07 (dd, ^3J=8.4 Hz, ^4J=2.5 Hz, 1H), 7.05 (d, J=7.8 Hz, 1H), 6.97 (t, J=7.8 Hz, 1H), 5.17 (s, 2H), 4.29 (m, 1H), 3.19 (s, 3H), 1.77 (m, 1H), 1.58 (m, 1H), 1.29 (m, 11H), 0.87 (m, 3H); ^{13}C NMR (100 MHz, $CDCl_3$) δ 190.1, 158.2, 152.7, 150.0, 147.5, 147.4, 137.9, 136.3, 123.9, 122.5, 121.2, 115.7, 112.8, 94.9, 77.9, 56.4, 36.8, 32.1, 29.5, 25.7, 22.9, 20.1, 14.4; MS (EI) m/z 386 (M^+, 9), 274 (36), 240 (100), 210 (60), 139 (50); HRMS (EI) calcd for $C_{23}H_{27}FO_4$: 386.1893, found 386.1898.

5.2.12. (*R*)-7-Methoxymethoxy-2-(2-octyloxy)-3-azafluoren-9-one (13b). The procedure described for the synthesis of **13a** was repeated with **12b** (0.480 g, 1.09 mmol) to give 261 mg (65%) of **13b** as an orange solid: m.p. 32–33°C (CH_2Cl_2/hexanes); IR (KBr) 1724 cm^{-1}; ^1H NMR (400 MHz, $CDCl_3$) δ 8.18 (s, 1H), 7.42 (d, J=8.1 Hz, 1H), 7.35 (d, J=2.2 Hz, 1H), 7.14 (dd, ^3J=8.1 Hz, ^4J=2.2 Hz, 1H), 6.87 (s, 1H), 5.18 (s, 2H), 5.16 (m, 1H), 3.48 (s, 3H), 1.57 (m, 13H), 0.86 (m, 3H) ; ^{13}C NMR (100 MHz, $CDCl_3$) δ 192.6, 167.8, 158.0, 144.9, 138.1, 137.7, 135.8, 130.0, 123.8, 121.6, 113.1, 107.8, 94.9, 73.1, 56.5, 36.5, 32.1, 29.6, 25.8, 22.9, 20.2, 14.4; MS (EI) m/z 369 (M^+, 2), 270 (4), 257 (12), 227 (6), 45 (100); HRMS (EI) calcd for $C_{22}H_{27}NO_4$: 369.1940, found 369.1932.

5.2.13. (*R*)-1-Fluoro-7-hydroxy-2-(2-octyloxy)fluoren-9-one (14a). To a solution of **13a** (1.49 g, 3.85 mmol) in *i*-PrOH (40 ml) was added 6M aq HCl (1.28 ml, 2.0 equiv). The mixture was stirred for 4 h at room temperature, diluted with water and the whole was extracted twice with CH_2Cl_2. The combined extracts were washed with brine, dried ($MgSO_4$) and concentrated to afford a red solid. Purification by flash chromatography on silica gel (10% EtOAc/hexanes) gave 0.98 g (74%) of **14a** as a dark red solid: m.p. 93–94°C (CH_2Cl_2/hexanes); IR (KBr) 3378, 1705 cm^{-1}; ^1H NMR (400 MHz, $CDCl_3$) δ 7.33 (s, 1H), 7.12 (d, J=2.8 Hz, 1H), 7.09 (s, 1H), 6.91 (m, 3H), 4.26 (m, 1H), 1.56 (m, 13H), 0.87 (m, 3H); ^{13}C NMR (100 MHz, $CDCl_3$) δ 191.6, 157.4, 152.7, 150.0, 147.1, 138.2, 136.5, 136.1, 124.1, 121.9, 121.6, 115.5, 112.4, 77.9, 36.7, 32.1, 29.6, 20.0, 14.4; MS (EI) m/z 342 (M^+, 18), 230 (100); HRMS (EI) calcd for $C_{21}H_{23}FO_3$: 342.1631, found 342.1637.

5.2.14. (*R*)-7-Hydroxy-2-(2-octyloxy)-3-azafluoren-9-one (14b). The procedure described for the synthesis of **14a** was repeated with **13b** (261 mg, 0.706 mmol) to give 223 mg (97%) of **14b** as a dark red solid: mp 135–136°C (CH_2Cl_2/hexanes); IR (KBr) 3313, 1709 cm^{-1}; ^1H NMR (400 MHz, $CDCl_3$) δ 8.11 (s, 1H), 7.67 (s, 1H), 7.31 (d, J=8.1 Hz, 1H), 7.17 (d, J=2.3 Hz, 1H), 6.99 (dd, ^3J=8.1 Hz, ^4J=2.3 Hz, 1H), 6.87 (s, 1H), 5.09 (m, 1H), 1.74 (m, 1H), 1.57 (m, 1H), 1.32 (m, 11H), 0.85 (m, 3H); ^{13}C NMR (100 MHz, $CDCl_3$) δ 193.4, 164.6, 157.3, 144.9, 137.2, 136.6, 135.8, 130.5, 123.1, 122.0, 112.6, 107.8, 73.6, 36.5, 32.1, 29.6, 25.7, 22.9, 20.1, 14.4; MS (EI) m/z 325 (M^+, 8), 294 (5), 213 (100), 196 (10), 185 (10); HRMS (EI) calcd for $C_{20}H_{23}NO_3$: 325.1678, found 325.1675.

5.2.15. (*R*)-1-Fluoro-2-(2-octyloxy)-7-(4-undecyloxybenzoyloxy)fluoren-9-one (2). A solution of **14a** (105 mg, 0.31 mmol), 4-octyloxybenzoic acid (98 mg, 1.1 equiv), DCC (69 mg, 1.1 equiv) and DMAP (4 mg, 0.10 equiv) in CH_2Cl_2 (5 ml) was stirred for 4 h at room temperature. The solution was poured over water and the whole was extracted twice with CH_2Cl_2. The combined organic extracts were dried ($MgSO_4$) and concentrated to give a yellow solid. Purification by flash chromatography on silica gel (10% EtOAc/hexanes) gave 148 mg (78%) of **2** as a yellow solid: IR (KBr) 1732, 1721 cm^{-1}; ^1H NMR (400 MHz, $CDCl_3$) δ 8.11 (d, J=8.8 Hz, 2H), 7.44 (m, 2H), 7.27 (dd, ^3J=7.8 Hz, ^4J=2.0 Hz, 1H), 7.14 (d, J=8.1 Hz, 1H), 7.01 (t, J=7.6 Hz, 1H), 6.96 (d, J=8.8 Hz, 2H), 4.33 (m, 1H), 4.03 (t, J=6.6 Hz, 2H), 1.82 (m, 2H), 1.38 (m, 29H), 0.88 (m, 6H); ^{13}C NMR (100 MHz, $CDCl^3$) δ 189.3, 164.9, 164.1, 152.5, 151.8, 149.9, 148.1, 141.5, 137.0, 136.0, 132.6, 128.0, 123.6, 121.0, 118.7, 116.4, 114.7, 77.8, 68.7, 32.2, 32.1, 29.9, 29.7, 19.6, 19.5, 19.4, 16.3, 15.7, 13.0, 22.9, 20.0, 14.4; MS (EI) m/z 616 (M^+, 5), 275 (100), 230 (9), 121 (45); HRMS (EI) calcd for $C_{39}H_{49}FO_5$: 616.3564, found 616.3532.

5.2.16. (*R*)-2-(2-Octyloxy)-7-(4-undecyloxybenzoyloxy)-3-azafluoren-9-one (3). The procedure described for the synthesis of **2** was repeated with **14b** (100 mg, 0.307 mmol) to give 172 m.g. (94%) of **3** as a yellow solid: IR (KBr) 1719, 1606 cm^{-1}; ^1H NMR (400 MHz, $CDCl_3$) δ 8.28 (s, 1H), 8.11 (d, J=8.9 Hz, 2H), 7.54 (d, J=8.1 Hz, 1H), 7.33 (d, J=2.2 Hz, 1H), 7.34 (dd, ^3J=8.1 Hz, ^4J=2.2 Hz, 1H), 6.96 (d, J=8.9 Hz, 2H), 6.91 (s, 1H), 5.21 (m, 1H), 4.03 (m, 2H), 1.79 (m, 3H), 1.57 (m, 1H), 1.33 (m, 27H), 0.88 (m, 6H); ^{13}C NMR (100 MHz, $CDCl_3$) δ 191.8, 165.2, 164.9, 164.1, 151.6, 144.8, 141.6, 138.6, 135.5, 132.7, 129.4, 129.0, 121.4, 121.2, 119.3, 114.7, 107.8, 73.2, 68.7, 36.5, 32.2, 32.1, 29.9, 29.7, 29.6, 29.4, 26.3, 25.8, 23.0, 22.9, 20.2, 14.4; MS (EI) m/z 600 (M^+, 3), 275 (100), 212 (9), 121 (60); HRMS (EI) calcd for $C_{38}H_{49}NO_5$: 599.3611, found 599.3644.

Acknowledgements

We are grateful to the Natural Sciences and Engineering Research Council of Canada, the Canada Foundation for Innovation and the Ontario Challenge Fund for support of this work.

References

[1] J.W. Goodby. In *Ferroelectric Liquid Crystals: Principles, Properties and Applications*, J.W. Goodby, R. Blinc, N.A. Clark, S.T. Lagerwall, M.A. Osipov, S.A. Pikin, T. Sakurai, K. Yoshino, B. Zeks (Eds), Gordon & Breach, Philadelphia. pp. 99–157 (1991).

[2] D.M. Walba. In *Advances in the Synthesis and Reactivity of Solids*, T.E. Mallouck (Ed.), JAI Press, Greenwich CT. p.173 (1991).

[3] (*a*) M.A. Glaser, N.A. Clark, D.M. Walba, M.P. Keyes, M.D. Radcliffe, D.C. Snustad, *Liq. Cryst.*, **29**, 1073 (2002); (*b*) M.A. Glaser. In *Advances in the Computer Simulations of Liquid Crystals*, C. Zannoni and P. Pasini (Eds), pp. 263–331. Kluwer, Dordrecht, The Netherlands (1999).

[4] D.M. Walba, M.B. Ros, N.A. Clark, R. Shao, M.G. Robinson, J.-Y. Liu, K.J. Johnson, D. Doroski. *J. Am. chem. Soc.*, **113**, 5471 (1991).

[5] M.D. Wand, R. Vohra, D.M. Walba, N.A. Clark, R. Shao. *Mol. Cryst. liq. Cryst.*, **202**, 183 (1991).

[6] W.K. Robinson, C. Carboni, P. Kloess, S. Perkins, H.J. Coles. *Liq. Cryst.*, **25**, 301 (1998).

[7] J. Naciri, J. Ruth, G. Crawford, R. Shashidhar, B.R. Ratna. *Chem. Mater.*, **7**, 1397 (1995).

[8] G.W. Gray, J.B. Hartley, A. Ibbotson, B. Jones. *J. chem. Soc.*, 4359 (1955).

[9] G.W. Gray, A. Ibbotson. *J. chem. Soc.*, 3228 (1957).

[10] K. Takatoh, K. Sunohara, M. Sakamoto. *Mol. Cryst. liq. Cryst.*, **164**, 167 (1988).

[11] K. Takatoh, M. Sakamoto. *Mol. Cryst. liq. Cryst.*, **182B**, 339 (1990).

[12] J.A. McCubbin, X. Tong, R. Wang, Y. Zhao, V. Snieckus, R.P. Lemieux. *J. Am. chem. Soc.*, **126**, 1161 (2004).

[13] M. Whisler, S. Macneil, V. Snieckus, P. Beak. *Angew. Chem. int. Ed.*, **43**, 2206 (2004).

[14] J.-M. Fu, B.P. Zhao, M.J. Sharp, V. Snieckus. *Can. J. Chem.*, **72**, 227 (1994).

[15] J.-M. Fu, B.P. Zhao, M.J. Sharp, V. Snieckus. *J. org. Chem.*, **56**, 1683 (1991).

[16] H.W. Gschwend, A. Hamdan. *J. org. Chem.*, **41**, 1173 (1982).

[17] W. Kuczynski, H. Stegemeyer. *Chem. Phys. Lett.*, **70**, 123 (1980).

[18] K. Miyasato, S. Abe, H. Takezoe, A. Fukuda, E. Kuze. *Jpn. J. appl. Phys.*, **22**, L661 (1983).

[19] P. Coutuner. *C. R.*, **202**, 1994 (1936).